Enhanced Non-Imaging Solar Concentrator for a Small Scale Drying in Buildings

Atul A. Sagade[1], Rodrigo Palma-Behnke[2,3], Edgar Estupiñan[1], Lorena Cornejo Ponce[1]

[1]Departamento de Ingeniería Mecánica, Universidad de Tarapacá, Arica (Chile)

[2] Energy Center, FCFM, University of Chile, Santiago (Chile)

[3]Dept. of Electrical Engineering, FCFM, University of Chile, Santiago (Chile)

Abstract

Building energy conservation technologies and developing green buildings have been essential priorities in the last decade. Building integrated clean cooking and heating systems using the Sun's energy can play a vital role in green buildings for several applications. This paper reveals the improved design of the prototype of non- imaging solar concentrator, named as BISC and its possible use for clean drying in buildings. The small prototype of the BISC is experimented under field conditions utilizing simplified thermal analysis for its performance.

The results show that the BISC able to achieve a temperature in the range of 59-74 °C, in the open drying operation. It ensures the potential for highly possible use in green buildings for drying with close drying operation, and other heating applications, such as cooking.

Keywords: sustainable development goals, green buildings and energy, Building integrated solar thermal technologies, solar drying, Renewable heating.

---

1. Introduction

Many building-integrated solar thermal collector systems (here onward denoted as BISTS) for heating have been reported in the past literature and have been popular from a long time (Morse, 1881; Fuschillo, 1975; Pierce, 1977). Diverse designs of concentrating BISTS were developed, which includes, roof integrated mini- parabolic solar collectors (Petrakis et al., 2009), Fresnel lens concentrator for cooling (Chemisana et al., 2013), and vertical heliostats (González-Pardo et al.,2014), and roof integrated two-stage solar concentrators (Bushra et al., 2022). Sultana et al., 2012 investigated concentrating semi-transparent BISTS in a novel rooftop solar micro-concentrating collector. Ratismith et al. 2014 proposed and compared (Ratismith et al. 2017) a tilted-tough collector arrangement with its orientation inwards at a 15° angle for heating application. The whole-day experimental results of the tilted-tough collector show an increase in efficiency of about 20% and could achieve apparent stagnation temperatures around ~ 180 °C, applicable for industrial process heat applications.

However, past literature significantly on BISTS lacks information about building-integrated solar dryers, even though the building-integrated solar thermal collectors showed good potential for heating and other applications but have not often been used for solar drying. On the contrary, solar drying has been one of the most favored fields of research for decades worldwide, and extensive literature is available on this topic. Interestingly and surprisingly, the investigators and designers of existing solar dryer designs did not keep an eye on their potential for large-scale building integration. There may be several reasons which could lead to the limited availability of literature and potential research gaps related to building integration of the solar dryers and can be enlisted as i) lack of interest and negligence of urban planners, building architects, and engineers as a potential technology for building energy conservation; ii) non-availability of appropriate designs of simple yet efficient building integrated solar dryers (hereafter denoted as BISD); iii) lack of attention, interest, and negligence by the research community to develop BISDs and their potential for low-

10.18086/swc.2023.06.09 Available at http://proceedings.ises.org

cost retrofitting, iv) very limited, rather unavailability of studies on the economics of BISDs v) lack of information about appropriate test methods, and thermal performance parameters available for performance evaluation of BISDs and their usefulness and appropriateness in testing BISDs, vi) lack of information about BISDs temperature attainment at a particular latitude(s) due to changes in solar geometry and weather conditions, even though building integrated solar thermal systems have the potential to reach intermediate to high temperatures (Bergmann and Weiß, 2002; Ratismith et al. 2017), vii) lack of appropriate design of BISDs for a particular latitude leading to apprehensions about their selection.

From the literature on building integrated solar thermal technologies; and most recent and existing designs of solar dryers (Sagade et al., 2022, 2023, Saxena et al. 2023), one can identify and understand the above-enlisted research gaps. Therefore, it is necessary to address them appropriately by presenting new and innovative designs for building integrated solar dryers. Hence, the present work aims to bridge the above-indicated research gap and demonstrate a prototype design of a non-tracking and non-imaging solar concentrator-based building integrated solar thermal dryer (BISD).

Thus, the novelty of the present work is i) design and build a primary prototype of the non-imaging and non-tracking compound parabolic solar concentrator-based BISD, ii) field experimentation of the BISD to demonstrate its usefulness, iii) determination of the thermal performance of the proposed BISD.

2. Materials and design of BISD

The BISD is an extended use of Building integrated solar thermal collector (BISTC) for drying application, which was previously used for cooking application (Sagade et al., 2023). However, detailed description is being avoided. The requirement of temperatures for drying process are relatively lower (~70 to 75 C). Therefore, the main change in the design of BISTC is removal of portable reflector used by Sagade at al. 2023. The reason for this design change is to i) reduced the temperatures in the absorber zone, which is used for drying process and ii) assess the heating performance ability of BISTC without portable reflector. Fig. 1a and 1b shows the photographs of test setup and BISD with drying material, respectively. and specifications are enlisted in Table 1.

Sr. no.	Component of BISD	Parameter
1.	waterproof plywood box	0.54 m (length) × 0.352 m (width) × 0.213 m (depth)
2.	dimensions of CPC are	0.46 m width, 0.35 m length, and 0.21 m depth,
3.	a rectangular absorber surface of CPC	0.23 m (width) × 0.35 m (length)
4.	Anodized aluminum reflectors used in CPC (ALANOD ® GmbH and Co.KG, Germany; Grade 320G)	Reflectivity = 0.86, thickness =0.3 mm
5.	The aperture and absorbing areas of CPC	0.161 m^2
6.	Absorbing area of CPC	0.08 m^2
7.	Effective inclined aperture area of CPC considering trapezoidal wall area	0.4 m^2
8.	The geometric concentration ratio (C_{gcr}) of BISD	2.012.
9.	Top and bottom lengths of the trapezoidal wall	1.08 m (top length); 0.54 m (bottom length)

BISD consists of a non-imaging compound parabolic concentrator (CPC) made of a galvanized iron sheet of 2 mm thickness is fitted in a plywood box. Anodized aluminum reflectors are glued over the galvanized iron surface of CPC, which acts as a reflecting surface of CPC. The building-integrated trapezoidal wall of the BISD is made of waterproof plywood and attached to one of the edges of a box, as shown in Fig. 1a. This allows handling the change in Sun elevation angle due to the Sun's motion over the given experimental day and season. This building-integrated trapezoidal wall is screwed with a anodized aluminum reflector, as mentioned above (See Fig. 1a), and acts as a booster reflector for the BISD. the heat absorbing area of CPC is coated with matt black paint.

The BISD was tested in a fixed position without providing any tracking. For this purpose, a trapezoidal wall faces south throughout the experiment at a location. However, the present work does not present any suggestions or guidelines about the architectural integration of the BISD.

Fig. 1a: Photograph of test setup for BISD

Fig.1b: Photograph of BISD with drying material (Sliced tomatoes)

3. Experiment and thermal analysis equations

Solar drying of the tomatoes has been done using BISD in the present work and drying performance is evaluated on the basis of the amount of moisture removed and the moisture removal rate from the drying material only. A black cloth is used to spread the drying products in the heat absorbing zone of BISD. The drying products (sliced tomatoes) of ~ 500g in the heat absorbing zone allowed to heat up under clear sun conditions without tracking of BISD, as indicated in Section 2. The solar flux falling on the CPC reflector and trapezoidal wall gets reflected in the heating zone of the BISD and food prodcut absorbs the heat. Thus, the temperature of heating zone rises slowly and gradually and moisure removal starts gradually.

A class 2 thermopile-type pyranometer (Dynalab, India) measures the total solar radiation (G_T) on the plane perpendicular to the beam radiation. The ambient air (T_a) and glycerin temperatures (T_{gly}) were measured using J-type temperature sensors. The wind sensor (Dynalab, India) measures the wind velocity at the experimental location. The windshield reduces the wind's impact during the experimentation. All the measuring instruments were connected to the data logger (UniLog, India), which records the experimental parameters every 90s.

The BISD was tested for its thermal performance in the window of ± 120 minutes of the solar noon to establish the primaty opto-thermal performance at the experimental location, SERL (17.66° N, 75.32° E) under ambient conditions as ($\bar{G_T}$) ≥ 700 W/m^2; 20˚C ≤ ($\bar{T_a}$) ≤ 40˚C and wind speed ≤ 1.5 m/s. However, the proposed BISD design may be applicable to the locations of latitude 0 to ± 23.5° around the globe, but such a study will be part of future work and not part of present investigations.

3.1 Thermal performance equations

3.1.1 Determination of moisture content for the solar drying cycle

Eq. 1 (Sethi et al. 2018) depicts the percentage of moisture content removed from the food products in BISD

$$Moisture\ content, (m_{wc}) = \frac{m_{di} - m_{df}}{m_{di}} \times 100\ (\%) \qquad (1)$$

where, m_{di} and m_{df} are the weight of food product before dehydration (kg), and after dehydration (kg), respectively.

3.1.2 Dehydration rate of the drying material for the drying cycle:

Eq. 2 (Sengar and Kurchania, 2005) expresses the dehydration rate of the drying material

$$Dehydration\ rate = \frac{m_{wc}}{\Delta t}\ \text{(kg/minute)} \qquad (2)$$

where, Δt is the time required for the drying .

3.1.3 Efficiency of the drying process in BISD

Eq. 3 (Andharia et al., 2022) shows the drying efficiency of BISD

$$\eta_D = \frac{Quantity\ of\ heat\ used\ in\ evaporating\ moisture}{solar\ flux\ incident\ on\ the\ BISD}$$

$$\eta_D = \frac{m_{wc} h_{fg}}{G_T A_p \Delta t}\ (\%) \qquad (3)$$

where, hfg is the latent heat of evaporating moisture is 2260 kJ/kg·K (Andharia et al., 2022))

4.Results and discussions

4.1 Drying performance of BISD

The present work establishes a proof of concept of the possible use of BISD using a prototype model and assess the performance at a temperature attainment in the drying process using non-tracking BISD. Fig. 2 depicts the variation of the different parameters observed for three (3) experimental days. In the drying cycle, on each experimental day, food products have the highest moisture content at the start of the test; thus, the reduction in moisture content is high at the initial phases and reduces gradually with drying time. BISD attains the temperatures in the range of 59-74 °C and can effectively dry a 500g of food products in the window of solar noon. The drying process removes a significant amount of moisture from the drying stuff. BISD removes ~95 to 96 % of moisture on different experimental days at a location during window of the solar noon. The use of cotton cloth below the drying products absorbs the considerable moisture and avoids the overheating and burning of the drying products. Obviously, drying is more efficient when the solar radiation is bright under clear weather.

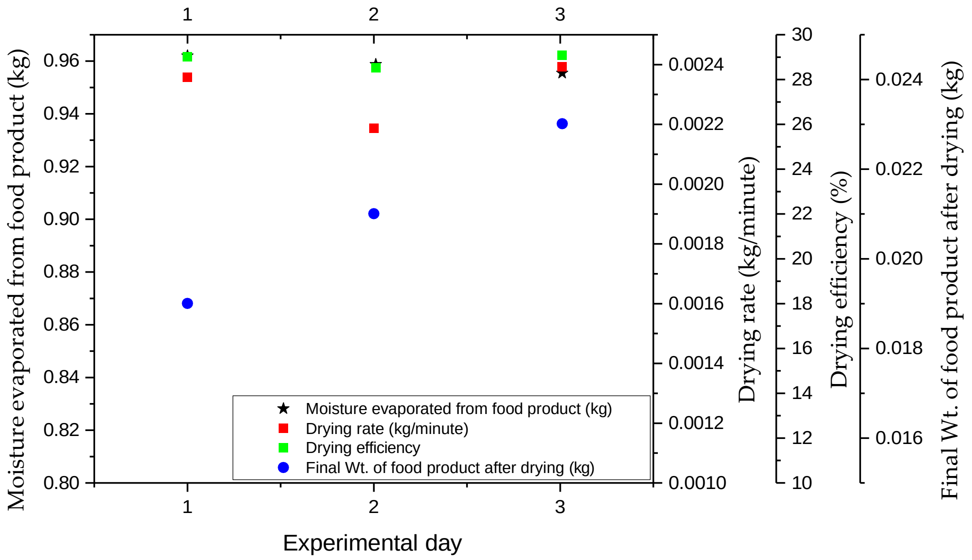

Fig. 2: Variation of experimental parameter for the drying process

Thus, the drying rate of the food products depends on solar radiation and the air temperature in the BISD's heating zone and is proportional to them. The drying rate of food products varies from 0.00218 to 0.00238 kg/minute on different experimental days. According to the variation of the ambient conditions, the dehydrating time was between 200-219 minutes. The higher the solar flux, higher is the drying rate of food products and maximum is reduction in the moisture content of the food product. Hence, at the end of the experiment on any typical day, the drying rate of food products slowed down and reached the apparent stagnation state where further moisture removal may not be possible.

Table 2: BISD's performance in the dehydration process

Day	($\bar{G}$) (W/m^2)	($\bar{T}_a$) (°C)	Initial Wt. of food product (kg)	Final Wt. of food product after drying (kg)	Moisture evaporated from food product (kg)	Drying time (minutes)	Drying rate (kg/minute)	Drying efficiency (%)
1	918	35.2	0.5	0.019	0.962	204	0.00235	29.02
2	869	36.8	0.5	0.021	0.958	219	0.00218	28.44
3	932	38.4	0.5	0.023	0.954	200	0.00238	28.91

The drying efficiency of the BISD is around of 29 % for all the three experiments at a location. Table 2 depicts the parameters used and determined for the drying process using BISD. Therefore, the reproducibility of the results confirms the usefulness of BISD as a potential design for small scale solar drying in buildings to avoid wastage of perishable food items. It also enables to preserve them by drying for later use.

5.Conclusions

The present work shows the proof of concept of non-tracking and non-imaging building integrated solar dryer. The major conclusions of the present investigations are summarized below

1. BISD removes ~95 to 96 % of moisture and cotton cloth enables to absorbs the considerable moisture and avoids the overheating and burning of the drying products.
2. The drying rate of food products varies from 0.00218 to 0.00238 kg/minute on different

experimental days.

3. The drying efficiency of the BISD is around of 29 % for all the three experiments at a location.
4. The present proof of concept of the BISD may be adapted for solar drying of different food products in decentralized energy sector with a possibility of their realistic integration in the buildings.
5. The reproducibility of the results confirms the usefulness of BISD for small scale solar drying in buildings.
6. Multiple use of the building integrated non-imaging and non-tracking CPC based solar concentrating collector is possible for at least two applications of cooking and drying the food products and can be extended for other several heating applications.

6.References

[1] Morse ES, Warming and Ventilating Apartments by the Sun's Rays Patent No. 246,626. 1881.
[2] Bergmann I, Weiß W. Fassadenintegration von thermischen Sonnenkollektoren ohne Hinterlüftung. Systemtechnische und bauphysikalische Grundlagen für die Fassadenintegration von thermischen Sonnenkollektoren ohne Hinterlüftung. Berichte aus der Enerige- und Umweltforschung. AEE Intec; Arbeitsgemeinschaft ERNEUERBARE ENERGIE; Institut für Nachhaltige Technologien, Gleisdorf. 2002.
[3] Petrakis M, Barakos G, Kaplanis S. Roof integrated mini-parabolic solar collectors. Comparison between simulation and experimental results. TOEFJ 2009;2 (1):71–81.
[4] Chemisana D, López-Villada J, Coronas A, Rosell JI, Lodi C. Building integration of concentrating systems for solar cooling applications. Appl Therm Eng 2013;50:1472–9. https://doi.org/10.1016/j.applthermaleng.2011.12.005.
[5] González-Pardo A, Rodríguez A, González-Aguilar J, Romero M. Analysis of solar shading caused by building-integrated Vertical Heliostat Fields. Energy Build 2014;76:199–210. https://doi.org/10.1016/j.enbuild.2014.02.009.
[6] Bushra N, Hartmann T, Constantin Ungureanu L. A method for global potential assessment of roof integrated two-stage solar concentrators (TSSCs) at district scale. Appl Energy 2022;326:120018. https://doi.org/10.1016/j.apenergy.2022.120018.
[7] Sultana T, Morrison GL, Rosengarten G. Thermal performance of a novel rooftop solar micro-concentrating collector. Solar Energy 2012;86:1992–2000. https://doi.org/10.1016/j.solener.2012.04.002.
[8] Ratismith W, Inthongkhum A, Briggs J. Two non-tracking solar collectors: Design criteria and performance analysis. Appl Energy 2014;131:201–10. https://doi.org/10.1016/j.apenergy.2014.06.030.
[9] Ratismith W, Favre Y, Canaff M, Briggs J. A non-tracking concentrating collector for solar thermal applications. Appl Energy 2017;200:39–46. https://doi.org/10.1016/j.apenergy.2017.05.044.
[10] Fuschillo, N., 1975. Semi-transparent solar collector window systems. Solar Energy 17, 159–165. https://doi.org/10.1016/0038-092X(75)90054-7
[11] Pierce, N. T. (1977). Massachusetts Institute of Technology US4143640 A
[12] Sagade, A.A., Palma-Behnke, R., 2023. Experimental feasibility study of multipurpose low-cost solar thermal device for different applications including inactivation of SARS CoV-2. Sustain. Energy Technol. Assess. 56, 103034 https://doi.org/10.1016/J.SETA.2023.103034.
[13] Sagade, A.A., Palma-Behnke, R., 2022. Novel design of the solar disinfectant closet (device) for inactivation of COVID-19 virus. p. 060005. https://doi.org/10.1063/5.0085676.
[14] Sagade, A.A., Sagade, N.A., Belgasim, B., Tawfik, M.A., Kulkarni, S., Shukla, S.K., 2023. Building integrated innovative non-imaging concentrating solar collector for clean cooking under low sun elevation. Sustain. Energy Technol. Assess. 57, 103234 https://doi.org/10.1016/j.seta.2023.103234.
[15] Saxena, A., Cuce, E., Singh, D.B., Sethi, M., Cuce, P.M., Sagade, A.A., Kumar, A., 2023. Experimental studies of latent heat storage based solar air heater for space heating: a comparative analysis. J. Build. Eng. 69, 106282 https://doi.org/10.1016/j.jobe.2023.106282